ESKİŞEHİR TEKNİK ÜNİVERSİTESİ BİLİM VE TEKNOLOJİ DERGİSİ
B- TEORİK BİLİMLER

Eskişehir Technical University Journal of Science and Technology B- Theoretical Sciences

International Conference on Natural Sciences and Technologies
Iconat Special Issue 2021

2021, Vol:9, pp. 74-84, DOI: 10.20290/estubtdb.1015146

ORBITAL INTERACTIONS AND STABILIZATION ENERGIES OF METHYL 5-6 DIHYDRO BENZO(H) QUINOLINE-4-CARBOXYLATE

Nihal KUŞ

Department of Physics, Science Faculty, Eskisehir Technical University, 26470, Eskisehir, Turkey

ABSTRACT

Quinolines are aromatic compounds consisting of benzene rings with a pyridine heterocyclic system. In this study, the structure and orbital interactions of the methyl 5-6 dihydro benzo(h) quinolone-4-carboxylate (MDQC) molecule, which is a quinoline derivative, were analyzed. In the calculation using the B3LYP/6-311++g(d,p) level, three conformers were found in the minimum energy state according to the O=C-O-C dihedral angle scan. The energy difference (ΔE+ZPV) between the conformers was calculated *ca*. 1.9 and 34.8 kJ mol^{-1}, respectively. The relative stability of the conformers was explained using the natural bond orbital (NBO) method and performed. The Fock matrix equation calculated donor and acceptor pairs and orbital energies for NBO pairs for the most stable conformer (MDQC-1). Dominant orbital interactions of selected NBOs for MDQC-1 were calculated at the theory level B3LYP/6-311++g(d,p) and plotted. The molecular electrostatic potential (MEP) surfaces were calculated by the DFT/B3LYP/6-311++g(d,p) method and drawn. NBO charges were calculated for MDQC-1 and MDQC-2 and analyzed.

Keywords: Methyl 5-6 dihydro benzo(h) quinolone-4-carboxylate, NBO, Orbital interaction, Stabilization energy

1. INTRODUCTION

Quinoline is a hetero-aromatic and organic compound with the formula C_9H_7N, which has a pyridine ring and a benzene ring attached to it. It is a colorless hygroscopic liquid with a pungent odor. It is very soluble in an organic solvent, but very slightly soluble in water. It decomposes rapidly in water and the atmosphere. Quinoline was first isolated by the German scientist chemist Friedlieb F. Runge. He was also the first to discover the caffeine compound in 1834 [1].

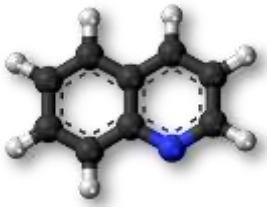

Quinoline (C_9H_7N)

Among heterocyclic compounds, quinoline and its derivatives is a heterocyclic compound that is being used in the development of new drugs. In addition, quinoline and its derivatives, which have many biological activities in the past and today, are also used in antimalarial drugs [2-8]. The quinine [(R)-(6-methoxyquinolin-4-yl)((2S,4S,8R)-8-vinylquinuclidin-2-yl)methanol] molecule, which is a quinoline derivative, is used in the treatment of malaria [9-10]. Nalidixic acid, the first member of this group of antibacterial agents, was produced in 1962 from the intermediate product obtained during the purification of chloroquine and is used as an antimalarial drug [11]. Quinoline, which is also used in optics, is also used in the paint and fungicide industries [12, 13]. Pharmacological quinolone derivatives

*Corresponding Author: nkus@eskisehir.edu.tr
Received: 26.10.2021 Published: 24.12.2021

are synthesized in the field of chemistry and have been used as an antibacterial agent since 1963. Quinolone derivatives (fluoroquinolones) are also used as antibiotic drugs [14]. Suitable several new synthesis methods for certain 4-hydroxyquinoline and 4-hydroxy-5,6-benzoquinoline derivatives have been developed and reported by Gould et al in 1939 [15]. No studies on the structure and properties of the MDQC molecule, which is the quinoline derivative we have studied, have not been encountered so far, and it has been researched and analyzed for the first time.

In previous studies, the molecular structure and physical properties of the quinoline derivatives, 5-hydroxyquinoline [16], 3-quinolinecarboxaldehyde [17], 4-chloro-7-iodoquinoline-3-carboxylate [18], 4-oxo-7-methyl quinoline-3-carboxylate, 4-Hydroxy-5-methyl quinoline-3-carboxylate [19] were experimentally elucidated by matrix isolation spectroscopy and reported with the support of theoretically using a computer program containing Density Functional Theory (DFT).

2. MATERIAL AND METHODS

The geometry optimization of the MDQC molecule and its minimum energy values were calculated using the B3LYP hybrid function of DFT and the 6-311++g(d,p) basis set. Gaussian 09 [20] computer program was used while making the calculations. B3LYP, which Becke describes the gradient change and programmed by Lee, Yang, and Parr, [21, 22] was used in all calculations. The orbital interaction, donor and acceptor energies, and natural charges of MDQC were calculated using NBO theory, considering the program integrated into Gaussian 09, designed by Weinhold et al. as NBO 3.1 [23]. The orbital interaction energies were calculated using the Fock matrix equation (*Eq.1*).

3. RESULTS AND DISCUSSION

Quinoline has two asymmetrical independent molecules in its crystal structure, determined at 150 K. In the crystal structure analysis, it was found to be monoclinic in the P21/c space group [24]. Quinoline derivative MDQC with the formula $C_{15}H_{13}NO_2$ is also called 5,6-dihydro-benzo[h]quinoline-4-carboxylic acid methyl ester. The conformers of the MDQC (MDQC-1, MDQC-2 and MDQC-3) were obtained by scanning the O=C−O−C dihedral angle in 15-degree steps, and it was optimized using DFT with B3LYP/6-311++g(d,p) basis set. The three different conformational energies in the minimum state were calculated are shown together with adopted atom numbers in Figure 1.

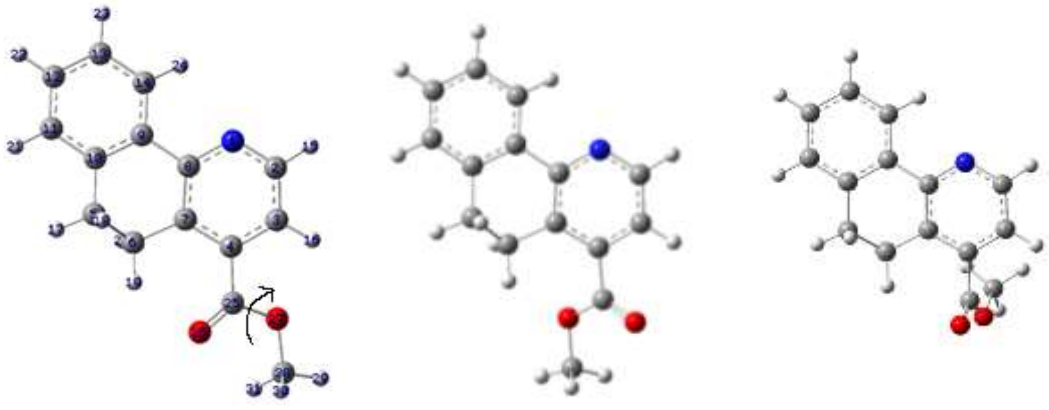

MDQC-1 MDQC-2 MDQC-3

Figure 1. Three conformers of MDQC with minimum energies calculated by DFT/B3LYP-6-311++g(d,p) level of theory. Color codes for O, C, H and N atoms are red, gray, white, and blue respectively.

With the rotation of the C−C−C−O dihedral angle, MDQC-1 and MDQC-2 conformations were obtained at minimum energy. In the present study, the results obtained by the C−O internal rotation of the aldehyde group were taken into account, and mostly the most stable form, MDQC-1, was emphasized. The calculated energies, energy differences for all possible conformers are given in Table 1. According to the calculations, MDQC-1 is more stable than the MDQC-2 and MDQC-3 by 2.05 and 36.47 kJ mol^{-1} (ΔE), with ΔE(0) = 1.88 and 34.47 kJ mol^{-1}, ΔG° = 2.95 and 33.02 kJ mol^{-1}, respectively. In a previous study on 3-furaldehyde, two conformers were found and the energy difference was 4.40 kJ mol^{-1} [25].

Table 1. Calculated electronic energies (with and without zero-point vibrational energy) and Gibbs energy for MDQC-1 and 2 using B3LYP/6-311++g(d,p) level.

Energy	MDQC-1	MDQC-2	MDQC-3
ΔE (kJ mol^{-1})	0	2.05	36.47
ΔE(ZPV) (kJ mol^{-1})	0	1.88	34.77
ΔG (kJ mol^{-1})	0	2.95	33.02
dipole (debye)	2.06	3.03	3.38

By scanning the dihedral angles C−C−C=O and O=C−O−C (or C−C−O=H) in 15-degree steps, two conformers with the same energy value in both scans, called trans and cis, were obtained. Since a third stable conformer was obtained when the O=C−O−C dihedral angle was scanned, the C−O rotation was taken into account and the potential energy profile was drawn and presented in Figure 2. In the figure, three conformers were located in the potential energy well. At the peaks, the shapes of the molecules in the transition state are drawn. In the figure, barrier energies and reverse energies are given. The calculated energy barrier for MDQC-1 and MDQC-3 is 52.12 kJ mol^{-1} and for MDQC-2 and MDQC-3 is 54.58 kJ mol^{-1}. The reverse process is 15.65 and 18.11 kJ mol^{-1}, respectively.

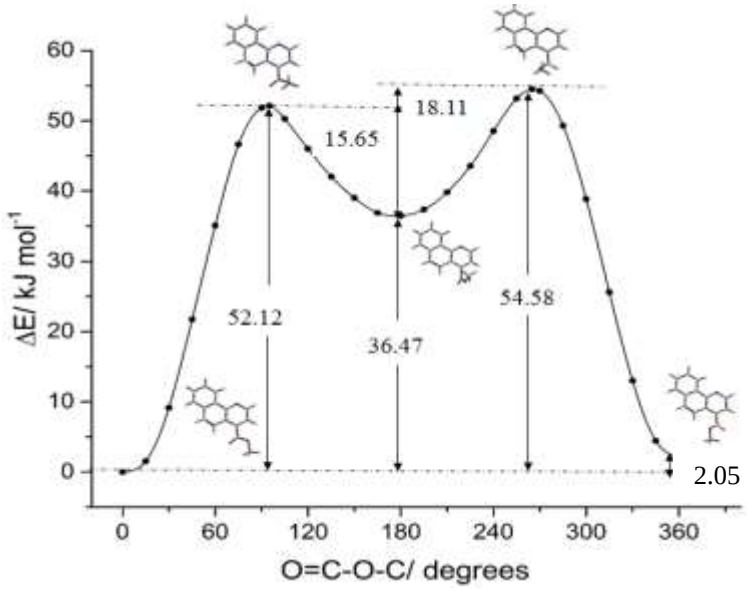

Figure 2. Potential energy profiles calculated by B3LYP/6-311++g(d,p) level for rotation about C–O bond for MDQC (atom numbers are given in Figure 1).

According to the value taken from the bottom of the potential well, the barrier energy calculated between the 1st and 3rd form is ~52.1 kJ mol^{-1}, while this value is only ~15.7 kJ mol^{-1} in the opposite direction. Likewise, while the barrier energy between the 2nd and 3rd form taken from the bottom of the potential well was ~54.6 kJ mol^{-1}, this value was found to be only ~18.1 kJ mol^{-1} in the opposite direction (Figure

2). Relative energies were calculated by rotating the C−O bond of the carboxylate group in 15-degree steps. When calculating the barrier energy, the possible dihedral angle of the molecule and the maximum peak were taken into account. O=C−O−C dihedral angles at the maximum point were found to be approximately 95 and 265 degrees, respectively.

Table 2. Donor and acceptor interactions and stabilization energies for NBO pairs results from calculated by the Fock matrix equation (Eq.1) for MDQC-1

Conformer	Pair	Donor NBO	Acceptor NBO	E(2)	e_j- e_i	F_{ij}
MDQC-1	A1	σ(C3−C4)	σ*(C25=O26)	9.66	1.30	0.049
	B1	σ(C4−C7)	σ*(C25−O27)	4.27	1.08	0.030
	C1	π(C4=C7)	π*(C25=O26)	66.52	0.28	0.062
	D1	σ(C4−C25)	σ*(C25=O26)	6.74	1.26	0.040
	E1	σ(C4−C25)	σ*(O27−C28)	15.94	0.93	0.053
	F1	σ(C7−C8)	σ*(C4−C25)	14.81	1.09	0.056
	G1	σ(C25−O26)	σ*(C3−C4)	3.77	1.65	0.035
	H1	σ(C25−O26)	σ*(C4−C25)	8.20	1.49	0.049
	J1	π(C25=O26)	π*(C4=C7)	10.71	0.50	0.035
	K1	σ(C25−O27)	σ*(C4−C7)	4.90	1.56	0.038
	L1	σ(O27−C28)	σ*(C4−C7)	6.65	1.45	0.043
	M1	σ(O27−C28)	σ*(C4−C25)	9.62	1.22	0.048
	N1	σ(O27−C28)	σ*(C5−C10)	3.72	1.30	0.030
	P1	σ(O27−C28)	σ*(C5−H17)	4.81	1.30	0.035
	Q1	σ(O27−C28)	σ*(C6−C7)	2.26	1.28	0.024
	R1	σ(O27−C28)	σ*(C6−H19)	33.55	1.82	0.108
	S1	σ(O27−C28)	σ*(C6−H20)	9.62	1.42	0.051
	T1	LP1(O26)	σ*(C4−C25)	10.38	1.11	0.047
	U1	LP2(O26)	σ*(C4−C25)	72.34	0.68	0.099
	V1	LP1(O27)	σ*(C4−C25)	2.47	0.98	0.033

In the present study, orbital interactions were analyzed for MDQC-1, which is in the most stable conformer state. In Table 2, stabilization energies related to the donor (Lewis)- acceptor (non-Lewis) interaction of the carboxylate group are given and calculated by the Fock matrix equation. It has been calculated that the C1 and U1 groups, which contribute the most to the stabilization energy, are caused by the π(C4=C7) donor - π*(C25−O26) acceptor and LP2(O26) donor-σ*(C4−C25) acceptor strongest interactions, respectively (Table 2). The orbital interaction energies were calculated using the Fock matrix equation given as *Eq.1* and stabilization energies are given in Table 2. Using the second-order perturbation approach, stabilization energies [*E (2)*] between donor-lone pairs and acceptor non-Lewis, Rydberg orbitals (filled and empty orbitals) were calculated [26].

$$E(2) = \Delta E_{ij} = q_i \frac{F_{ij}^2}{\varepsilon_j - \varepsilon_i} \qquad (Eq.1)$$

In *Eq.1*, q_i is the donor orbital occupancy, ε_i and ε_j are the diagonal elements and F_{ij} is NBO the off-diagonal NBO Fock matrix element.

As can be seen in Table 2, the strongest stabilization exhibited from LP2(O26) to (C4−C25) bond and they were hybridized sigma characters. While π bond was observed in the oxygen, σ bond was observed from the interaction of C4 and C25.

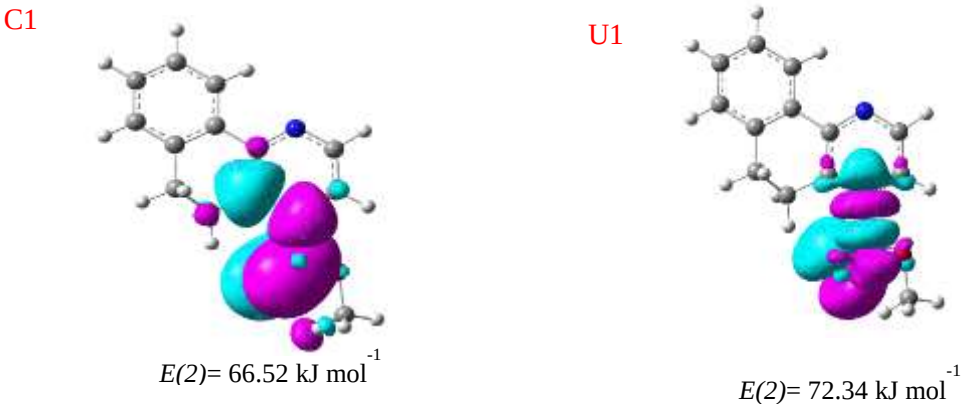

Figure 3. Orbital interaction scheme with the highest stabilization energy related to the carboxylate group

The total s-type energy (U1) is 72.34 kJ mol^{-1} for MDQC-1 (Figure 3). This interaction is known as the back donation effect, from oxygen lone electron pair (especially p-type lone pair; LP2) to C4−C25 bonds. Back donation from the O to the CO increases, one would expect the C−C to bond becomes stronger and the C=O bond becomes weaker. Thus, the changes in bond order should be demonstrated by shorter C−C and longer C=O bonds compared to C−C single bonds and C=O double bonds, respectively.

Figure 4 shows the selected dominant orbital interactions scheme for NBOs of interest to the corresponding carboxylate group related to electron density calculated at the B3LYP/6 311++g(d,p) level. For isovalues of electron densities, 0.02 *e* is taken into account. Blue and magenta colors indicate the states of positive and negative wave function signs, respectively.

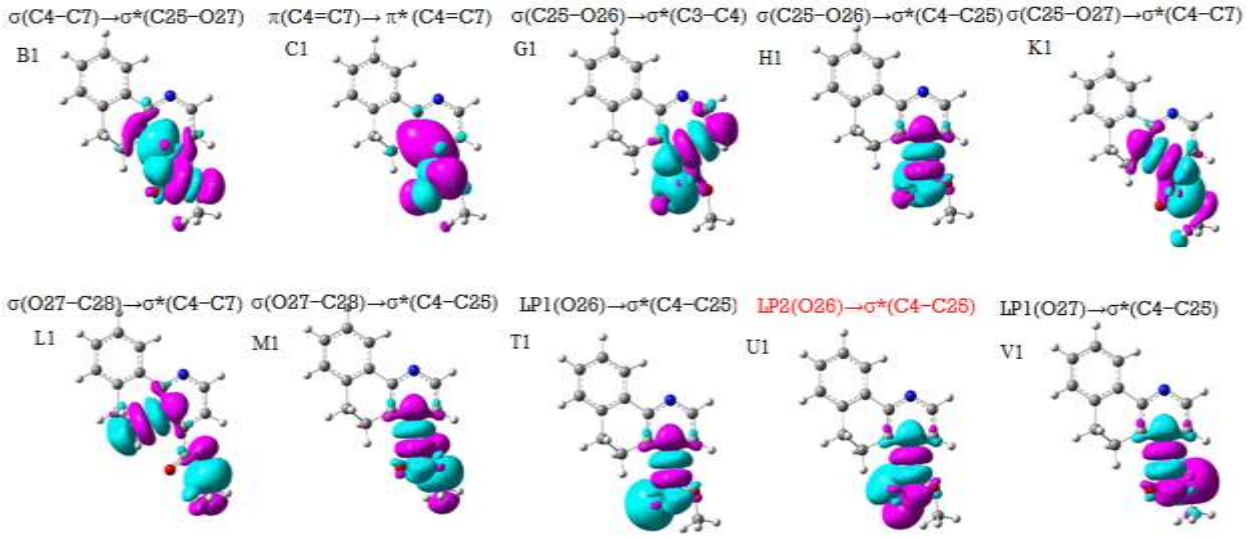

Figure 4. Selected dominant orbital interactions for MDQC-1 of the carboxylate group.

Selected stabilization energies, the occupancy ratio of the bond orbitals, NBO coefficients of the atoms and their hybridizations are given in Table 3. This Table also presents the bonding percentage of atomic orbitals in each atom, subtracted from the NBO polarization coefficients for NBO orbitals.

Table 3. Orbitals, occupancy, coefficients, and hybridization for MDQC-1, calculated using B3LYP/6-311++g(d,p) level.

Group	NBO	Occupancy Ratio	Coeficients (%)[a]		Hybridization[b]
			A	B	
Donor	σ(C3−C4)	1.97148	48.49	51.51	$0.6963sp^{1.86} + 0.7177sp^{1.87}$
	σ(C4−C7)	1.97002	50.82	49.18	$0.7129sp^{1.75} + 0.7013sp^{1.85}$
	π(C4=C7)	1.63187	52.49	47.51	0.7245p + 0.6893p
	σ(C4−C25)	1.97296	51.56	48.44	$0.7180sp^{2.46} + 0.6960sp^{1.57}$
	σ(C7−C8)	1.97226	50.37	49.63	$0.7097sp^{2.04} + 0.7045sp^{1.73}$
	σ(C25=O26)	1.99524	35.04	64.96	$0.5919sp^{1.96} + 0.8060sp^{1.46}$
	π(C25=O26)	1.98393	29.96	70.04	0.5474p + 0.8369p
	σ(C25−O27)	1.99295	31.19	68.81	$0.5585sp^{2.68} + 0.8295sp^{2.05}$
	σ(O27−C28)	1.99133	69.35	30.65	$0.8327sp^{2.53} + 0.5537sp^{3.78}$
	LP1(O26)	1.97751			$sp^{0.69}$
	LP2(O26)	1.84766			p

[a] Percent contribution of each atom.
[b] Definition of hybrid orbitals.

Group	NBO	Occupancy Ratio	Coeficients (%)[a]		Hybridization[b]
			A	B	
Acceptor	σ*(C25=O26)	0.02036	64.96	35.04	$0.8060sp^{1.96} - 0.5919sp^{1.46}$
	σ*(C25−O27)	0.09936	68.81	31.1	$0.8295sp^{2.68} - 0.5585sp^{2.05}$
	π*(C25=O26)	0.24257	70.04	29.9	0.8369p - 0.5474p
	σ*(O27−C28)	0.01616	30.65	69.35	$0.5537sp^{2.53} - 0.8327sp^{3.78}$
	σ*(C4−C25)	0.06484	48.44	51.56	$0.6960sp^{2.46} - 0.7180sp^{1.57}$
	σ*(C3−C4)	0.02084	51.51	48.49	$0.7177sp^{1.86} - 0.6963sp^{1.87}$
	π*(C4=C7)	0.34532	47.51	52.49	0.6893p - 0.7245p
	σ*(C4−C7)	0.02775	49.18	50.82	$0.7013sp^{1.75} - 0.7129sp^{1.85}$
	σ*(C5−C10)	0.02222	50.53	49.47	$0.7108sp^{2.49} - 0.7034sp^{2.23}$
	σ*(C5−H17)	0.01101	39.49	60.51	$0.6284sp^{3.45} - 0.7779s$
	σ*(C6−C7)	0.02323	51.59	48.41	$0.7183sp^{2.67} - 0.6957sp^{2.12}$
	σ*(C6−H19)	0.01379	37.52	62.48	$0.6125sp^{3.17} - 0.7904s$
	σ*(C6−H20)	0.01859	39.54	60.46	$0.6288sp^{3.72} - 0.7776s$
	LP1(O27)	1.96475			$sp^{1.57}$

All anti-bonding orbitals cause weak delocalization and make no comparative contribution to occupancies NBOs. According to the NBO interactions, most of the orbital interactions belonging to the carboxylate group of the molecule have strong sp hybridization.

Table 4. Total Lewis and non-Lewis occupancies (valence, core, and Rydberg shells). (e=1.60217646×10^{-19} C)

	MDQC-1	MDQC-2	MDQC-3
Core	35.98464*e* (99.957% of 36)	35.98487*e* (99.958% of 36)	35.98457*e* (99.957% of 36)
Valence Lewis	86.68312*e* (96.315% of 90)	86.68934*e* (96.321% of 90)	86.49269*e* (96.103% of 90)
Total Lewis	**122.66777*e* (97.355% of 126)**	**122.67421*e* (97.360% of 126)**	**122.47726*e* (97.204% of 126)**
Valence non-Lewis	3.06582*e* (2.433% of 126)	3.06192*e* (2.430% of 126)	3.22682*e* (2.561% of 126)
Rydberg non-Lewis	0.26641*e* (0.211% of 126)	0.26388*e* (0.209% of 126)	0.29592*e* (0.235% of 126)
Total non-Lewis	**3.33223*e* (2.645% of 126)**	**3.32579*e* (2.640% of 126)**	**3.52274*e* (2.796% of 126)**

The A and B values in Table 3 are obtained from the polarization coefficients. It forms a bond for the NBO orbitals of the atomic orbitals of the two atoms corresponding to the contributions of the atoms forming the pairs. The electron densities between the donor and acceptor orbitals depend on the Lewis and non-Lewis NBO orbitals.

In Table 4, the nuclei, valence and Rydberg occupancy percentages of Lewis and non-Lewis bonded orbitals calculated for the three conformers at minimum energy are given. Total Lewis and non-Lewis were calculated 97.355% and 2.645% for MDQC-1, 97.360% and 2.6407% for MDQC-2 and 97.204% and 2.796% for MDQC-3.

HOMO energy, which represents the electron-donating ability of the molecule, is related to the ionization potential. The LUMO energy represents the ability of the molecule to accept electrons. In the calculation at the B3LYP/6-311++g(d,p) level of theory, it was found that the interacting HOMO-LUMO orbitals of the MDQC-1 were closer to each other than the other conformers ($\Delta E_{HOMO\text{-}LUMO}$= 4.31 eV). In this case, the interaction and reaction of the reactants occur more easily and MDQC-1 is less reactive than the other two conformers. Figure5 shows the HOMO-LUMO energy ranges and orbital interaction diagram.

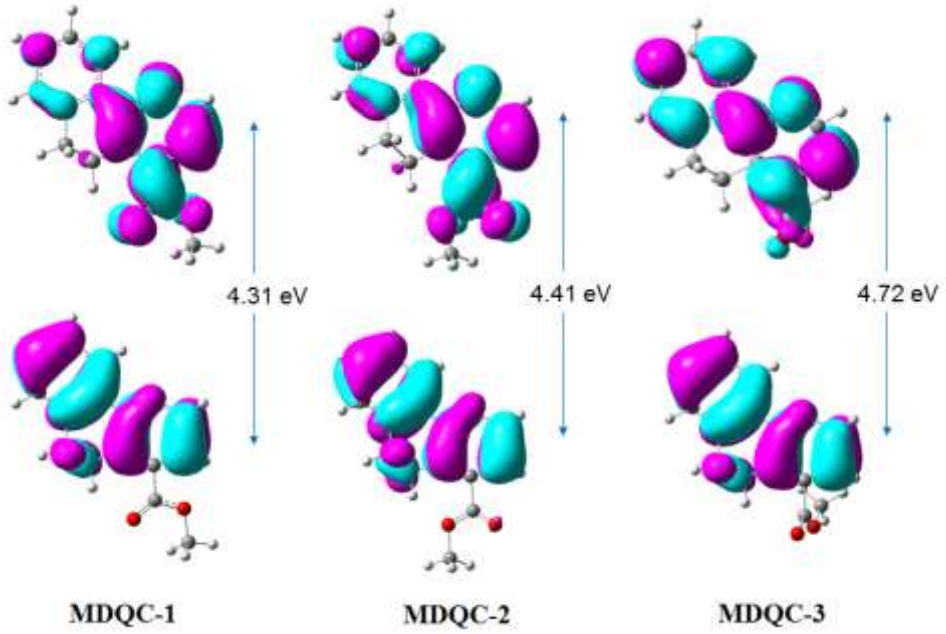

Figure 5. HOMO-LUMO energy gap for MDQC conformers

It is seen that the HOMO orbital is localized on the rings in all three conformations, while the LUMO orbital is mostly localized on the phenyl rings.

The natural charges for MDQC-1 and MDQC-2 are given in Figure 6. The dipole interactions can be related to the strongly polarized C25−O26 bond in the molecule (for MDQC-1 charges on C25 and O26 are of +0.805*e* and -0.595*e*, and for MDQC-2 +0.802*e* and -0.549*e*, respectively).

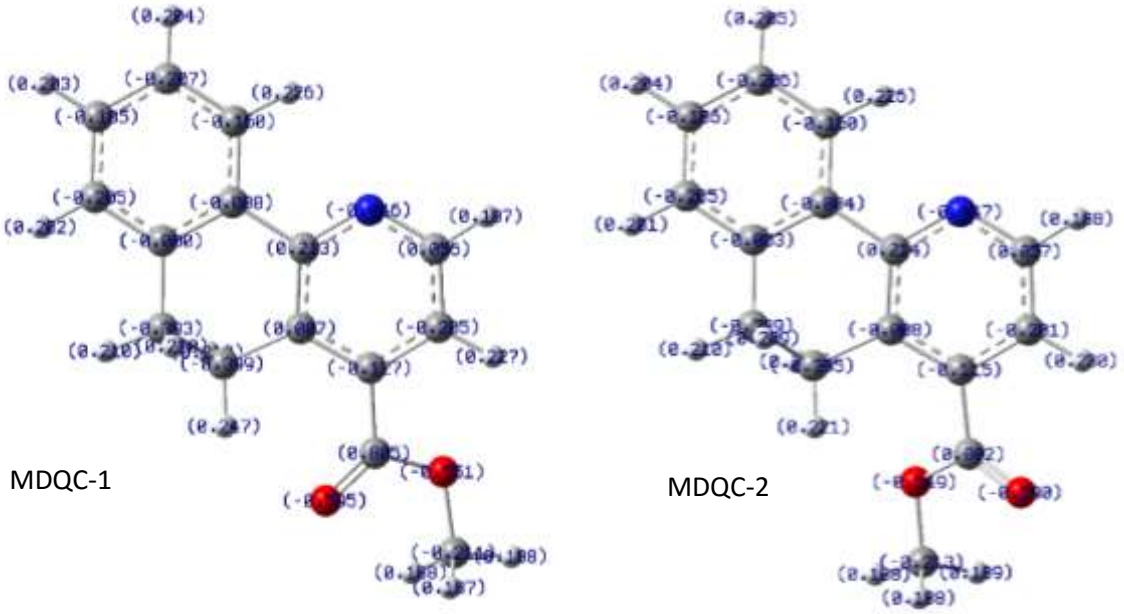

Figure 6. Natural atomic charges for MDQC-1 and MDQC-2 calculated by DFT/B3LYP/6-311++g(d,p) level of theory

Electron density calculated for MDQC-1 and MDQC-2 is given with color codes and surface maps of molecular electrostatic potential (MEP) are shown in Figure 7. The MEP map shows the approximate maximum distance the electron density can reach for MDQC-1 and 2 (also known as the Van der Waals surface).

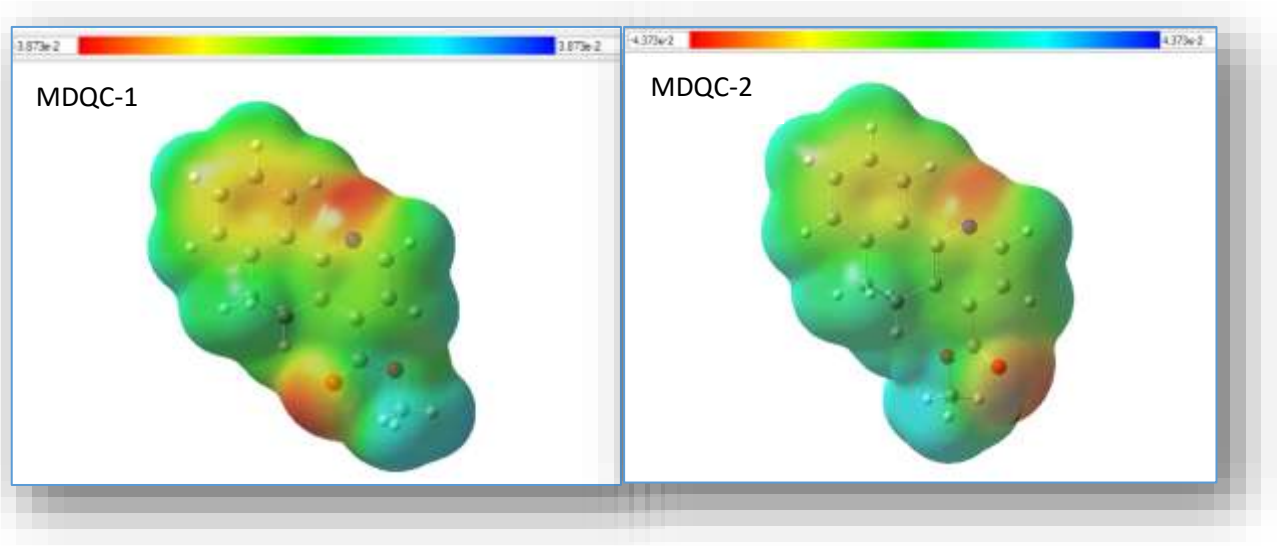

Figure 7. MEP surface for MDQC-1 and 2

MEPs of MDQC-1 and MDQC-2 were drawn using GaussView5 visualization program. MEP surfaces visualize charge regions of the molecule. On the MEP map, the most negative potential (the region with higher electron density over the entire molecule than the nucleus) is shown in red, while blue is used to show the most positive potential (the region with partial positive charges). These values are between -

3.873e-2 (max. red region) and +3.873e-2 (max. blue region) for MDQC-1 and between -4.373e-2 (max. red region) and +4.373e-2 (max. blue region) for MDQC-2. The map showed that the negative electrostatic potentials (red region, electrophilic attack) were intensified around the O26 atom while the maximum electrostatic potential (blue region, nucleophilic attack) was intensified around the CH3 methyl group hydrogens for MDQC-1 and 2. From Figure 7, it can be seen that between O26 and C25 atoms attraction is more concentrated.

4. CONCLUSIONS

The conformers of MDQC were calculated in the ground electronic state using DFT/B3LYP/6-311++g(d,p) level of theory. MDQC-1 was more stable than the MDQC-2 conformer *ca.* 2.05 kJ mol^{-1}. Orbital interaction energies, electron density surfaces and hybridizations of MDQC-1 related carboxylate group were determined using B3LYP/6-311++g(d,p) level using NBO method. Effective orbital interactions of the carboxylate group were analyzed and discussed. It was seen that Back donation effect was observed from LP2(O26) to σ*(C4−C25). The HOMO-LUMO energy gap was calculated for all conformers. For MDQC-1, it was found to be the smallest at *ca.* 4.3 eV. According to the natural charge distribution on the atoms and the MEP map, the negative electrostatic potential region was observed around the oxygen and nitrogen atoms, while the positive potential region was observed around the methyl group hydrogen atoms for MDQC-1 and MDQC-2.

ACKNOWLEDGMENT

This work was supported by the Eskisehir Technical University Commission of Research Project under grant no: 20ADP144.

CONFLICT OF INTEREST

The authors stated that there are no conflicts of interest regarding the publication of this article.

REFERENCES

[1] Foley M, Tilley L. Quinoline Antimalarials: Mechanisms of Action and Resistance and Prospects for New Agents. Pharmacol Ther 1998;79: 55−87.

[2] Acton QA, Ed Antimalarial Quinolines: Advances in Research and Application, 2012 ed.; Scholarly Eds: Atlanta, GA, USA, 2013.

[3] Vlok MC. Artemisinin-Quinoline Hybrids: Design, Synthesis and Antimalarial Activity. Ph.D. Thesis, North-West University, Potchefstroom, 2013.

[4] Vargas LY, Castelli MV, Kouznetsov VV, Urbina JM, Lopez SN, Sortino M, Enriz RD, Ribas JC, Zacchino S. In vitro Antifungal Activity of New Series of Homoallylamines and Related Compounds with Inhibitory Properties of the Synthesis of Fungal Cell Wall Polymers. Bioorg Med Chem 2003; 11: 1531−1550.

[5] Ablordeppey SY, Fan P, Li S, Clark AM, Hufford CD. Substituted Indoloquinolines as New Antifungal Agents. Bioorg Med Chem 2002; 10: 1337−1346.

[6] Madapa S, Tusi Z, Batra S. Advances in the Synthesis of Quinoline and Quinoline-Annulated Ring Systems Curr Org Chem 2008; 12: 1116−1183.

[7] Vandekerckhove S and D'hooghe M. Quinoline-based antimalarial hybrid compounds. Bioorg Med Chem 2015; 23: 5098–5119.

[8] Lyon MA, Lawrence S, William JD and Jackson YA. Synthesis and structure verification of an analog of kuanoniamine. A J Chem Soc Perkin Trans 1999; 1: 437–442.

[9] World Health Organization. Guidelines for the Treatment of Malaria, Second ed; World Health Organization: Geneva, 2010.

[10] Dorndorp A, Nosten F, Stepniewska K, Day N, White N. South East Asian Quinine Artesunate Malaria Trial (SEAQUAMAT) Group. Artesunate versus Quinine for Treatment of Severe Falciparum Malaria: A Randomised Trial Lancet 2005; 366: 717−25.

[11] Gregory SB. Origins of the Quinolone Class of Antibacterials: An Expanded "Discovery Story. J Med Chem 2015; 58(12): 4874–4882.

[12] Całus S, Gondek E, Danel A, Jarosz B, Pokładko M, Kityk AV. Electro-luminescence of 6-R-1,3-diphenyl-1H-Pyrazolo[3,4-b]quinoline-based Organic Light-Emitting Diodes (R= F, Br, Cl, CH3, C2H3 and N(C6H5)2). Mater Lett 2007; 61: 3292−3295.

[13] Caeiro G, Lopes JM, Magnoux P, Ayrault P and Ramoa Ribeiro FJ. A FT-IR Study of Deactivation Phenomena in Catalytic Cracking: Nitrogen Poisoning, Coke Formation, and Acidity-activity.Correlations. J Catal 2007; 249: 234−243.

[14] Paton JH, Reeves DS. Fluoroquinolone antibiotics. Microbiology, pharmacokinetics, and clinical use. Drugs. 1988; 36(2): 193−228.

[15] Gordon GR and Walter AJ. Synthesis of Substituted Quinolines and 5,6-Benzoquinolines. J Am Chem Soc 1939; 61; 2890−2895.

[16] Kuş N, Sagdinc S, Fausto R. Infrared Spectrum and UV-Induced Photochemistry of Matrix-Isolated 5-Hydroxyquinoline. J Phys Chem A 2015; 119(24): 6296−308.

[17] Kuş N, Henriques MS, Paixão JS, Lapinski L, and Fausto R. Crystal Structure, Matrix-Isolation FTIR, and UV-Induced Conformational Isomerization of 3-Quinolinecarboxaldehyde. J Phys Chem A 2014; 118 (38): 8708−8716.

[18] Horta P, Henriques MSC, Kuş N, Paixão JA, O'Neill PM, Cristiano MLS, Fausto R. Synthesis, structural and conformational analysis, and IR spectra of ethyl 4-chloro-7-iodoquinoline-3-carboxylate. Tetrahedron 2015; 71: 7583−7592.

[19] Horta P, Kuş N, Henriques MS, Paixão JA, Coelho L, Nogueira F, O'Neill PM, Fausto R, Cristiano ML. Quinolone-Hydroxyquinoline Tautomerism in Quinolone 3-Esters. Preserving the 4-Oxoquinoline Structure to Retain Antimalarial Activity. J Org Chem 2015; 80(24): 12244−57.

[20] Frisch MJ et al. Gaussian 09, Revision A.0.2. Gaussian Inc, Wallingford CT, 2009.

[21] Becke AD. Density-functional exchange-energy approximation with correct asymptotic behavior, Phys Rev A 1988; 38: 3098−3100.

[22] Lee C, Yang W, Parr RG. Development of the Colle-Salvetti correlation-energy formula into a functional of the electron density. Phys Rev B 1988; 37: 785−789.

[23] Reed AE, Curtiss LA, Weinhold F. Intermolecular interactions from a natural bond orbital, donor-acceptor viewpoint. Chem Rev 1988; 88: 899−926.

[24] Davies JE, Andrew DB. Quinoline. Acta Cryst 2001; E57: o947−o949.

[25] Kuş N, Reva I, Fausto R. Photoisomerization and photochemistry of matrix-isolated 3-furaldehyde. J Phys Chem A 2010; 114(47): 12427−36.

[26] Weinhold F, Landis CR. Valency and Bonding. A Natural Bond Orbital Donor-Acceptor Perspective. Cambridge University Press: New York, 2005.